The 2009 IEEE/RSJ International Conference on
Intelligent Robots and Systems
October 11-15, 2009 St. Louis, USA

Development of a Remote Trauma Care Assist Robot

Mark W. Noakes, *Member, IEEE*, Randall F. Lind, John F. Jansen, *Member, IEEE*, Lonnie J. Love, *Member, IEEE*, François G. Pin, and Bradley S. Richardson

***Abstract*—In typical teleoperated surgeries, skilled staff are still necessary in the remote surgical room to change manipulator tooling and to manage surgical supply delivery and removal. This paper describes the development of a nurse robot to provide automated support to a teleoperated surgical manipulator system in environments where the presence of skilled surgical support staff may not be practical. The tools must be inserted precisely into a compliant manipulator in a timely manner, and the supplies are diverse in nature. To support experimental investigations and evaluations, a seven degrees-of-freedom commercially available manipulator was selected. The design of novel end-effecters, tool grasping and supply holding features, and tool auto-loading systems for optimum surgical tool changing and supply delivery in minimum time is presented. A novel approach for calibration of the nurse robot among compliant and rigid subsystems and for managing forces during subsystem interaction is described and experimental results using this force management approach are presented. Overall experimental performance data for the nurse robot system during tool changing and supply delivery tasks is also presented to illustrate the feasibility of performing these functions in a remote medical or trauma care-assist cell.**

***Index Terms*—Multiple end-effecters, nurse robot, surgical robot, telesurgery, smart tooling.**

I. INTRODUCTION

THIS paper describes a nurse robot capable of automatically changing tools on a compliant surgical teleoperator and addresses the calibration and system-to-system mechanical interface issues required to make automatic tool change feasible. A secondary feature of the nurse robot is the ability to quickly deliver and remove surgical supplies to and from the surgical site. While these tasks are accomplished with a commercial seven degree-of-freedom (DOF) robot manipulator, significant technical challenges must be overcome to permit successful operation. The objective of this research was to develop the enabling capabilities and demonstrate the feasibility of robotic interaction with a compliant teleoperator for automated tool changing and supply delivery.

In typical teleoperated surgeries—though it is now possible for the surgeon to be located a great distance away—skilled support staff must still be present in the operating room to change manipulator tooling and to manage surgical supply delivery and removal. However, there are environments and situations, such as rural or remote medical facilities, where the presence of medical support staff may not be practical. By automating the support staff functions that service the teleoperated surgical manipulators, a more autonomous telesurgery capability is generated. However, achieving greater independence from human support introduces significant challenges: the surgical tools must be inserted precisely into the compliant surgical teleoperator on command in a timely manner; supplies that are diverse in nature must be delivered and removed from the surgical site; time constraints and reliability of supply delivery and tool insertion become critical issues; and calibration must be addressed for all the interacting subsystems.

Nurse robots have been investigated as early as the 1980s, however, mostly as service robots to tend to patients needs upon request. Borenstein and Koren provided some of the earliest work along these lines with mobile platform algorithms for unstructured environments [1]. While the sophistication of the hardware and basic motion capabilities have changed, typical nurse robots are still similar in their service focus and function, as expressed by Shieh et al. with their interactive nurse robot to tend to children [2].

Research on surgical nurse robots has primarily focused on support to the surgeon instead of interaction with a teleoperated surgical manipulator. Kochan outlines the development of the Penelope scrub nurse robot, designed to hand tools to the surgeon and track the large number of surgical supplies used in a typical operation [3]. In order to address a shortage of nurses in Japan, Miyawaki, Yoshimitsu, and Sadahiro have also pursued the development of a robotic scrub nurse system that can hand surgical tools to the surgeon and retrieve them back from the surgeon [4], [5], [6]. The focus is human interaction with robot systems at varying surgeon capability levels.

Research in telesurgery dates to the late 1980s. Charles et al. proposed design guidelines and operating constraints for "telemicrorobotics" [7]. Green reported on the SRI systems [8], [9], the technology of which was based on the force-reflecting servo-manipulator concept first proposed by Goertz for nuclear materials handling [10]. The kinematics of the manipulator system, however, was optimized for minimally

This work was supported in part by the U.S. Department of Energy (DOE) Laboratory Directed Research and Development Program and by the Defense Advanced Research Projects Agency (DARPA) under Inter-Federal Agency Agreement No. 1868-HH00-X1 with the U.S. DOE.

M. W. Noakes is with the Oak Ridge National Laboratory (ORNL), Oak Ridge, TN 37831-6305 USA (phone: 865-574-5695; fax: 865-574-4624; e-mail: noakesmw@ornl.gov). ORNL is managed by UT-Battelle for the U.S. Department of Energy under contract DE-AC05-00OR22725.

R. F. Lind is with the Oak Ridge National Laboratory, Oak Ridge, TN 37831-6305 USE (e-mail: lindrf@ornl.gov).

J. F. Jansen is with the Oak Ridge National Laboratory, Oak Ridge, TN 37831-6305 USE (e-mail: jansenjf@ornl.gov).

L. J. Love is with the Oak Ridge National Laboratory, Oak Ridge, TN 37831-6305 USE (e-mail: lovelj@ornl.gov).

F. G. Pin is with the Oak Ridge National Laboratory, Oak Ridge, TN 37831-6305 USE (e-mail: pinfg@ornl.gov).

B. S. Richardson is with the Oak Ridge National Laboratory, Oak Ridge, TN 37831-6305 USE (e-mail: richardsonbs@ornl.gov).

invasive laparoscopic surgery. Taylor et al. also outlined an early laparoscopic surgical telerobotics assistant [11]. In this case the goal was to provide a third hand. Schenker et al. developed a prototype system [12] with focus on microsurgery and tremor control at the limits of human dexterity. Madhani et al. developed the Black Falcon, an 8-DOF teleoperator, for minimally invasive surgery [13]. The most prolific and now commercially available laparoscopic surgical teleoperator is the da Vinci system by Intuitive Surgical, Inc. [14], [15]. Due to its wide use and acceptance in the surgical field, it was selected as the experimental telesurgical system to support the work presented in this paper on the nurse robot. The work described here has been part of a larger project funded by the Defense Advanced Research Projects Agency to develop a remote robotic cell, called TraumaPod, containing surgical and trauma care systems to stabilize wounded soldiers. The overall system, which also applies to the concept of the "Operating Room of the Future," [16] has been previously described by Garcia et al. [17]. This paper focuses on the details of the nurse robot and its interactions with the various other subsystems within the remote surgical site. The next section describes the basic nurse robot and the unique subsystems that were developed to support automated tool exchange and supply delivery. Section 3 addresses the force sensing, calibration, and control algorithms that were developed to ensure proper interaction between the robotics and teleoperated manipulators in the surgical cell. Experimental results in tasks involving tool change are then presented with our conclusions.

II. System Description

A. Scrub Nurse Robot

Basic requirements for the nurse robot included a payload on the order of 10 kg (including the dual end-effecter and force-torque sensor), a reach of 1 meter or more, maximum end-effecter velocities on the order of 1 m/s, and 7 DOF for axes of manipulation. The degrees of freedom were driven by the need for obstacle avoidance in the operating area while maintaining 6 DOF at the end-effecter. A commercially available system was desired and, after a study of the various parameters was conducted, the Mitsubishi PA10-7C manipulator was selected.

The PA10 shown in Fig. 1 is an AC servomotor-driven 7-DOF manipulator with the joints specified as (from the base to the tool plate at the end-effecter) revolute (R) – pitch (P) – R – P – R – P – R. The bottom R – P – R joints are considered shoulder joints; the elbow joints are P – R; and the distal joints P – R are the final wrist joints. Joint velocities vary from 1 rad/sec at the base joints to 2 rad/sec at the distal joints.

The PA10 uses a proprietary controller that includes a separate interface to a PCI card that mounts in a host PC. As such the controller configuration cannot be modified and must be accessed with high-level commands.

B. Dual End-Effecter

Multiple gripper manipulator systems and their efficiencies have received little attention to date in research. Sethi et al. verified the productivity advantage of dual-gripper systems for pick and place operations [18]. For the surgical nurse robot, a study of task time requirements determined that a dual-gripper end-effecter could significantly speed up tool changes and supply deliveries. The final design, supplied by the University of Washington, placed the two grippers side by side in the same horizontal plane as shown in Fig. 2. This allowed the nurse robot to pick up a tool, move to the da Vinci manipulator, remove an existing tool and insert the new tool without first returning the removed tool, and then return the removed tool to storage, thereby saving two long motions within the cell.

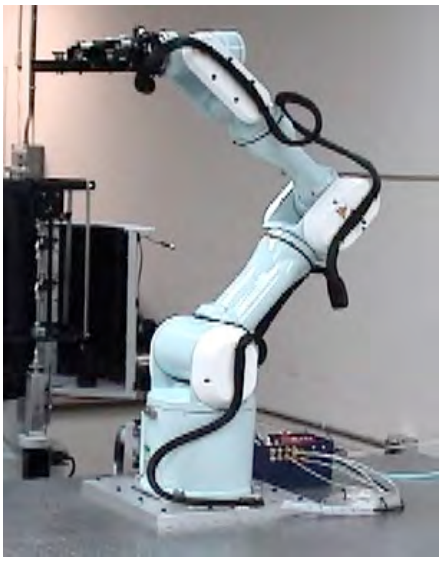

Fig. 1. Mitsubishi PA10-7C 7-DOF nurse robot.

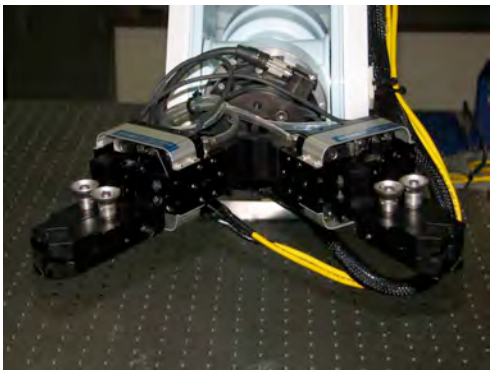

Fig. 2. Dual pneumatic end-effecter for the nurse robot.

As described in the next section, the gripper fingers were specifically designed to match and grasp a specially designed lug, which was used on the tools, the calibration lug, and the supply trays, further increasing the reliability and accuracy of the acquisition tasks and speeding processes by avoiding any change of end-effecter. To support the force-based grasp and insertion control, an ATI Gamma series force/torque sensor was mounted between the tool plate of the PA10 manipulator and the base mount of the dual end-effecter (see Fig. 2). With no need for articulated manipulation between full-open and full-closed positions, pneumatic-actuated grippers were used, which allowed reduced mass of the end-effecter (half the initial electric design concept) and actuation time of less than .3 sec.

C. Tool Autoloader

The most crucial task for the nurse robot to execute is to change tools on the da Vinci surgical system teleoperated manipulators. The da Vinci tools are designed to be installed by a human hand and the da Vinci tool receiver mechanism relies on extensive human tactile feedback and cognizance to place and properly seat the tool. A typical tool, shown being inserted in Fig. 3, consists of a body housing an interface chassis, a 4-DOF disk-based actuation interface to the da Vinci, an electrical interface to the da Vinci, and the manipulation shaft and end-effecter that extend down into the patient. A typical tool is about 50-cm long with a shaft diameter of about 8 mm, and weighs about 160 gm. Tool insertion must manage insertion of the shaft into a cannula while also inserting the body of the tool into a receiver on the surgical manipulator, while allowing the four disk actuators to synchronize and the electrical contacts to properly mate up, all without jamming. As originally designed this is a difficult task to automate. Even highly trained nurses and technicians sometimes have to seat the tool more than once before it can be acquired correctly by the da Vinci control system. Additionally, the design of the tool body is such that a robot manipulator cannot grasp the tool securely. Thus, both the method and the mechanisms for handling and changing the tools had to be modified to support greater reliability and suitability for robotics operations, and a smart tooling approach [19] was utilized.

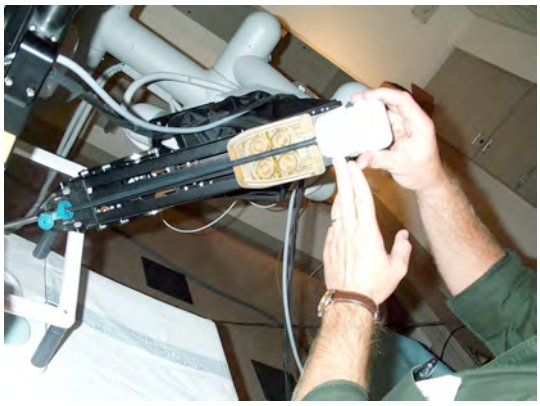

Fig. 3. Unmodified da Vinci surgical tool during manual insertion.

The tool cover on the da Vinci tools was replaced as shown in Fig. 4 with a custom grasp lug that permits the robot to firmly grasp the tool and hold it rigidly in 6 DOF. The lug, in conjunction with the gripper fingers, is specifically designed using geometric reasoning to provide self-centering in all 6 DOF, while also allowing significant initial grasp misalignment. A similar grasp feature was used on the thermo-molded trays that were used to carry the wide variety of surgical supplies. These may consist of sponges, small absorbent blankets, sutures, or any one of a number of small tools, and must be presented to the surgeon in such a way that they can be picked up efficiently. Spent supplies must also be collected and accounted for so that nothing is accidentally left in the patient after the operation. Thus, trays were found to be the most expedient method to store the wide configuration of sterile supplies, move them around the surgical cell, and present them to the surgeon for pick-up or disposal. As discussed later, the calibration lug is based on the same design, with the addition of programmed structural compliance for position and orientation deflection.

Fig. 4. Modified tool cover for robust end-effecter grasping.

The tool receiver on the da Vinci was replaced with a clamping insertion-based design that accepted the tool straight in. Two flippers closed on the specially designed cover to hold it firmly in place. To accommodate a design that could receive a tool straight in rather than in a sliding motion, the original cannula was replaced with a clamping cannula design that could open and close on command. The new tool receiver, clamping cannula, and a modified tool are shown installed on a da Vinci in Fig. 5. To estimate the required chamfers on the tool receiver and tray receiver devices in order to compensate for possible misalignment, the range of position and orientation errors at the target points were established through error stack-ups and repeatability data for the da Vinci and the PA10, and through testing of the robot manipulator operating at high velocity. This led to chamfer sizes designed to guarantee 100% capture on all interactions, contingent to proper calibration of the various subsystems with respect to each other.

III. Calibration, Force Control, and Managing Subsystem Interaction Contact

As discussed in the previous section, the various components are designed to accommodate reasonable positional errors through the use of well-designed chamfers and compliance; however, they cannot accommodate large errors resulting from setup. A force-based approach was adopted to calibrate the nurse robot to minimize the interaction insertion forces.

This calibration procedure is based upon a “force zeroing” concept that consists of grasping a compliant lug, reading the forces imparted to the robot by grasping the lug and transforming those forces into an incremental move to reduce the forces to an acceptable threshold. These steps are then repeated until the force is reduced to a preset limit or until a maximum number of iterations is reached. The key element of this approach is the compliant calibration lug shown in Figs. 6 and 7. As mentioned previously, the lug is designed to allow large initial misalignment between the

manipulator and the calibration points. The lug compliance allows for a fairly straightforward analysis to assess contact instability limits due to force feedback. Lug compliance was programmed by experimental testing to roughly match that of the da Vinci manipulators. Prototypes were fabricated via fast prototyping printer, and tested for performance.

Fig. 5. Complete tool autoloader during early testing.

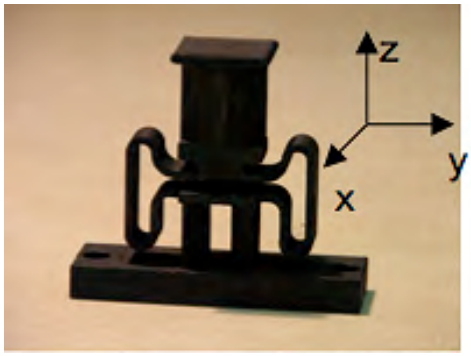

Fig. 6. Compliant calibration lug.

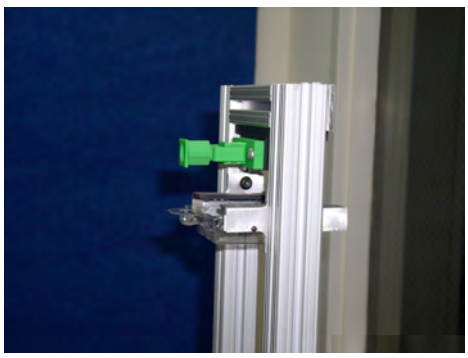

Fig. 7. Calibration lug and supply tray test stand.

It is well known that when a robotic manipulator makes contact with the environment while employing some form of force control, electromechanical instabilities are possible and typically take the form of a limit cycle where the robot is making and breaking contact with the workplace [20], [21]. To avoid possible limit cycles, a dynamic analysis was undertaken to obtain a fundamental understanding of the salient gain magnitudes of the force feedback signal. This information provided the initial analysis to design the compliance for the calibration lug and to set the initial bounds for the feedback gain that was then optimized experimentally. Figure 8 shows a 3-DOF rigid body diagram of a simplified joint of the PA10 in contact with the environment. The spring constants are represented by the k_i terms, the damping effects by the b_i terms, the effective masses by the m_i terms, and the displacements by the x_i terms. The three rigid bodies represent the robot, the force sensor and the work piece. The actuator force is represented by an F source.

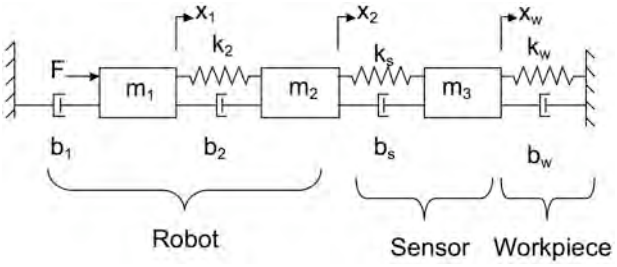

Fig. 8. Robotic model including work piece dynamics.

The compliance for the calibration lugs has been measured as 9.6 N/m in the x and y directions and 14.0 N/m in the z direction with the directions shown in Fig. 6. Because the compliance of the calibration lugs is so low, the dynamic model of the system including the work piece can be drastically simplified to the one shown in Fig. 9.

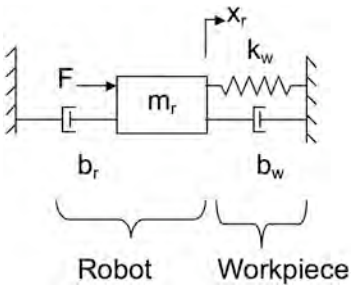

Fig. 9. Robotic model including work piece dynamics.

The transfer function of the system in Fig. 9 is a 2nd order system represented by

$$\frac{x_r}{F}(s) = \frac{1}{m_r s^2 + (b_s + b_r)s + k_w} \qquad (1)$$

The position control block diagram is shown in Fig. 10 where the feedback gain, K_p, is adjusted along with the other model constants to obtain an approximate 2nd order model of the dynamic response of each joint.

As mentioned by other authors, the system in Fig. 10 is intrinsically stable [20], [21]. Next, an outer feedback loop using an accommodation-based formulation of force is inserted around the position control loop as shown in Fig. 11. The system shown in Fig. 11 can be made unstable if the accommodation gain, α, is made too large because the order of the system has increased from 2nd to a 3rd with a time delay term associated with the sampler. The sampling block can be modeled as a standard sample and hold element, i.e., $\left(1-e^{-sT_s}\right)/s$, where T_s is running at 0.01 seconds.

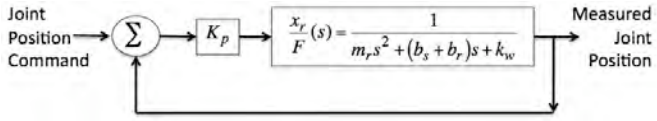

Fig. 10. Robot position controller.

The characteristic equation for the system in Fig. 10 is:

$$m_r s^4 + (b_w + b_r)s^3 + (k_w + K_p)s^2 + K_p \alpha k_w (1 - e^{-sT_s}) = 0 \quad (2)$$

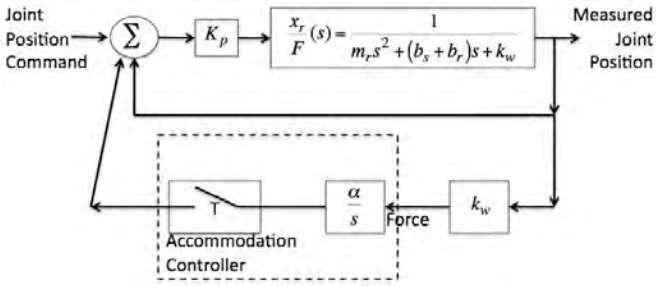

Fig. 11. Outer loop accommodation with nondeterministic sample rate, T.

While a root locus plot of Eq. (2) can be performed, an additional simplification can be made that allows for deeper insight into the problem. Based on experience with the PA10, the electromechanical bandwidth of the manipulator using the compliant calibration lug is less than 1 Hz. The phase shift due to the sample and hold (using T_s = 0.01 sec) at 1 Hz is less than 2 degrees of phase lag, which means that the delay in the sampler can be ignored. The characteristic equation then simplifies to

$$m_r s^3 + (b_w + b_r)s^2 + (k_w + K_p)s + K_p \alpha k_w = 0 \quad (3)$$

and, employing the Routh's stability criterion, the accommodation feedback gain bound is

$$\begin{aligned} \alpha &< \frac{(b_r + b_w)(k_w + K_p)}{m_r k_w K_p} = \frac{(2m_r \omega_r \xi_n)}{k_w K_p} \frac{(k_w + K_p)}{m_r} \\ &< \frac{(2m_r \omega_n \xi_n)}{k_w K_p} \omega_{n^2} = \frac{2\omega_{n^3} \xi_n}{k_w} \frac{m_r}{K_p} < \frac{2\omega_n \xi_n}{k_w} \end{aligned} \quad (4)$$

where the relationships for the natural frequency $\omega_n = \sqrt{(k_w + K_p)/m_r} > \sqrt{K_p/m_r}$ and damping $\xi_n = (b_r + b_w)/2m_r\omega_n$ have been utilized, and we have bounded the values of ω_n to be under 6.2 rad/sec, ξ_n to be around 0.7, and k_w no greater than 14 N/m. We started with a value of α around 1% of the maximum bound and adjusted the gain upward until satisfactory performance was obtained. The point of the previous development was not a rigorous stability analysis but rather to bound the initial force feedback gain that was used in further experimental refinement and to provide input to the design of the calibration lug. This was especially important when interacting with easily damaged, delicate, and expensive equipment.

The force-zeroing algorithm includes a number of provisions to enhance its utility. For safety reasons, motion along each axis was limited to maximum translations of 2 mm and rotations of 2.9 degrees per iteration, thus requiring multiple iterations in nearly all cases.

Gains and threshold forces and moments were determined and set for the primary calibration configurations. Stiffness of the lug and the subsystem to which it was attached was the primary consideration. As anticipated, the force zeroing converged much more rapidly for the stiffer subsystems. Through careful selection of the gains, adequate performance was also achieved on the more compliant subsystems such as the da Vinci surgical manipulator that used grasp of the tool lug as a calibration point instead of using the flexible calibration lug. The maximum number of iterations was set at 20, which provided sufficient margin for convergence for all subsystem calibrations.

The most stringent requirement for the force-based algorithms was that less than 1-lb force could be imparted on the da Vinci surgical manipulator during tool insertion/extraction. Thus, a scheme to monitor and limit the forces to a task-dependent limit was implemented. The ATI 6-axis force sensor was sampled every 10 ms through the real-time control system, which is operating at 100 Hz. At arm speeds of 1 m/s, the arm moves a maximum of 1 cm per cycle (10 ms), while at contact approach velocities of 10 cm/s the arm moves 1 mm every cycle. At these slower speeds, the dynamic of the arm is low and, therefore, the force limits at which an immediate stop is issued can be chosen based upon the amount of compliance of the subsystem contacted. Since compliance of each subsystem is known, the force-limiting algorithm applied at each control cycle provides adequate protection for the hardware. As stated previously, during tool changes, the amount of allowable force imparted on the da Vinci was the limiting case. During free-space motions the limit is set high to avoid an error due to inertial loads.

IV. Results and Conclusion

A specific requirement for the nurse robot was that design and controls during insertion and removal tasks should limit any force that could damage delicate equipment. During the experimental program, these forces and moments resulting from the design of the tools, trays and autoloader concept were measured by testing prototypical insertions with the PA10 while recording data from the force/torque sensor.

Typical plots of unfiltered raw force and moment data for the *Z*-axis during development are shown in Figs. 12 and 13. The initial transition spikes are of such short duration (10 ms) that they are beyond the bandwidth of the manipulator and so were discounted. There was no specification on moment so attempts were made to quantify and minimize its effect. With the maximum expected position error of 4 mm and the maximum expected rotational misalignment of 2 degrees in the receiving equipment, final measurements showed maximum forces to be less than 1 lb on transition with static forces well within the requirements of less than one-pound force on the da Vinci arms:

X-axis: F_x = 3.70N (.83lbs); M_x = .96N-m (.71 ft-lb)
Y-axis: F_y = 1.78N (.40lbs); M_y = .92N-m (.68 ft-lb)
Z-axis: F_z = 1.59N (.36lbs); M_z = .30N-m (.22 ft-lb)

In summary, the combination of the lugs for accurate grasping and self-centering, chamfers on the receiving devices and on the autoloader, the build-in compliance, the force-based calibration concept, and the force-limiting algorithm have proven to be extremely efficient and reliable in accomplishing the difficult autonomous insertion and retrieval tasks on the delicate and compliant surgical arms, and very adequate approaches for protecting the delicate hardware during contact operations.

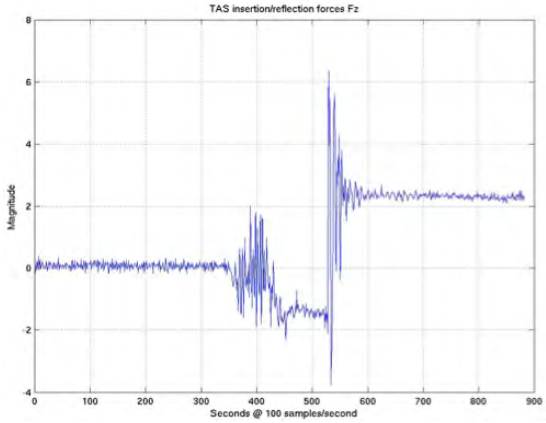

Fig. 12. Test for maximum insertion force F_z (in N).

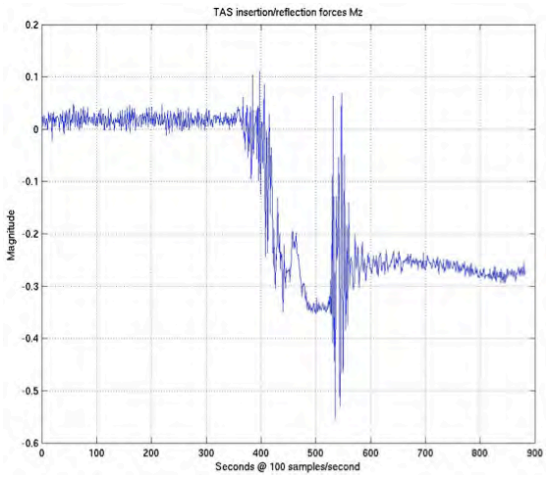

Fig. 13. Test for maximum insertion moment M_z (in N-m).

REFERENCES

[1] J. Borenstein and Y. Koren, "A mobile platform for nursing robots," *IEEE Transactions on Industrial Electronics*, vol. IE-32, no. 2, pp. 158-165, May 1985.

[2] M. Y. Shieh, C. M. Lu, C. C. Chen, C. Y. Chuang, and Y. S. Lai, "Design and implementation of an interactive nurse robot," in *Proc. SICE 2007 Annual Conference*, Sept. 17-20, 2007, pp.2121–2125.

[3] A. Kochan, "Scapel please, robot: Penelope's debut in the operating room," *Industrial Robot: An International Journal*, vol. 32, no. 6, pp. 449–451, 2005.

[4] F. Miyawaki, "Scrub nurse robot system-interoperative motion analysis of a scrub nurse and timed-automata-based model for surgery, *IEEE Trans. on Industrial Electronics*, vol. 52, no. 5, October 2005, pp. 1227–1235.

[5] K. Yoshimitsu et al., "Development and evaluation of the second version of scrub nurse robot (SNR) for endoscopic and laparoscopic surgery," in *Proc. IEEE/RSJ International Conference on Intelligent Robots and Systems*, 2007 (IROS 2007), Oct. 29–Nov. 2, 2007, pp. 2288–2294.

[6] T. Sadahiro et al., "Laparoscopic skill measurement with COP to realize a HAM scrub nurse robot system," in *Proc. IEEE International Conference on Systems, Man, and Cybernetics 2007*, Oct. 7–10, 2007, pp. 2983-2988.

[7] S. Charles, R. E. Williams, and W. R. Hamel, "Design of a surgeon-machine interface for teleoperated microsurgery," in *Proc. Annual International Conference of the IEEE Engineering in Medicine and Biology Society*, vol. 3, Nov. 9–12, pp. 883–884, 1989.

[8] P. S. Green, "Advanced teleoperator technology for enhanced minimally invasive surgery," in *Proc. of Medicine Meets Virtual Reality Conference*, San Diego, June 4–7, 1992.

[9] P. S. Green, J. W. Hill, J. F. Jensen, and A. Shah, "Telepresence surgery," *IEEE Engineering in Medicine and Biology Magazine*, vol. 14, no. 3, May/June 1995, pp. 324-329.

[10] R. Goertz and F. Bevilacqua, "A force-reflecting positional servomechanism," Nucleonics, vol. 10, no. 11, pp. 43–45, 1952.

[11] R. H. Taylor et al., "A telerobotic assistant for laparoscopic surgery," *IEEE Engineering in Medicine and Biology Magazine*, vol. 14, no. 3, May/June 1995, pp. 279-288.

[12] P. Schenker, H. Das, and T. R. Ohm, "Development of a new high-dexterity manipulator for robot-assisted microsurgery," in *Proc. SPIE*, vol. 2351, 191, Nov. 1, 1994.

[13] A. J. Madhani, G. Niemeyer, and J. K. K. Salisbury, Jr., "The black falcon: a teleoperated surgical instrument for minimally invasive surgery," in *Proc. 1998 IEEE/RSJ International Conference on Intelligent Robots and Systems*, vol. 2, Oct 13–17, 1998, pp. 936–944.

[14] G. S. Guthart et al., The Intuitive Telesurgery System: Overview and Application, in *Proc. 2000 IEEE ICRA*, 2000, pp. 618–621.

[15] Intuitive Surgical, http://www.intuitivesurgical.com/corporate/index.aspx, 2005.

[16] R. M. Satava, "Disruptive visions: operating room of the future, *Surgical Endoscopy*, vol. 17, no. 1, pp. 104-107, 2003.

[17] P. Garcia et al., "Trauma pod: a semi-automated telerobotic surgical system," *The International Journal of Medical Robotics and Computer Assisted Surgery* **5**(2), 136–146 (2009).

[18] S. P. Sethi, J. B. Sidney, and C. Sriskandarajah, "Scheduling in dual gripper robotic cells for productivity gains," *IEEE Transactions on Robotics and Automation*, vol. 17, no. 3, June 2001, pp. 324–341.

[19] P. Dario, B. Hannaford, and A Menciassi, "Smart surgical tools and augmentating devices," *IEEE Transactions on Robotics and Automation*, vol. 19, no. 5, Oct. 2003, pp. 782–792.

[20] S. D. Eppinger and W. P. Seering, "Introduction to dynamic models for robot force control," *IEEE Control Magazine*, April 1987, pp. 48–52.

[21] S. D. Eppinger and W. P. Seering, "On dynamic models for robot force control," in *Proc. 1986 IEEE International Conference on Robotics and Automation*, Vol. 3, April 1, 1986.